Recent progress with the BYU/NRAO phased array feed

BYU
BRIGHAM YOUNG UNIVERSITY

Brian D. Jeffs, Karl F. Warnick, Jonathan Landon, Michael Elmer
Department of Electrical and Computer Engineering
Brigham Young University, Provo, UT

J. Richard Fisher and Roger Norrod
National Radio Astronomy Observatory
Green Bank, West Virginia

CALIM 2009, Socorro New Mexico
March 30 – April 3, 2009

Array Feed Development Efforts

- Apertif (Astron, The Netherlands)
- PHAD (DRAO, Canada)
- ASKAP (CSIRO, Australia)
- BYU/NRAO Centimeter Band PAF (U.S.) (Green Bank and Arecibo)

Design Challenges

- Broadband
  - Near term single reflector PAFs: 300 to 500 MHz bandwidth at L-band
  - SKA goal: 500-1500MHz (3:1)
- High sensitivity
  - 80% aperture efficiency, >99% radiation efficiency
  - System temperature below 50 Kelvin at L-band
  - Mutual coupling
- Low SNR (-30 to -50 dB)
- Stable gain for radiometric detection
- High dynamic range - weak fields near bright sources and stable, well characterized sidelobes
- Immunity to radio frequency interference (RFI)
- Modeling and characterization

⇒ Radio astronomy is pushing phased array technology into a new regime!
⇒ New area of R&D for antenna designers…

BYU/NRAO L-Band PAFs

2006:

- 7 element hexagonal single-pol dipole array on 3m reflector
- Array signal processing studies
- RFI mitigation experiments

Nov. 2007:

- 19 element single-pol dipole array on Green Bank 20-Meter Telescope
- Electromagnetically simple elements
- ~1 MHz instantaneous bandwidth
- Real time multichannel data acquisition
- 150 K T_{sys}
- First demonstration of on-reflector PAF

July/August 2008:

- 19 element dipole array
- 33 K LNAs (room temperature)
- 1.3 – 1.7 MHz tunable bandwidth
- *Goal: highest possible sensitivity*
- 66 K T_{sys}

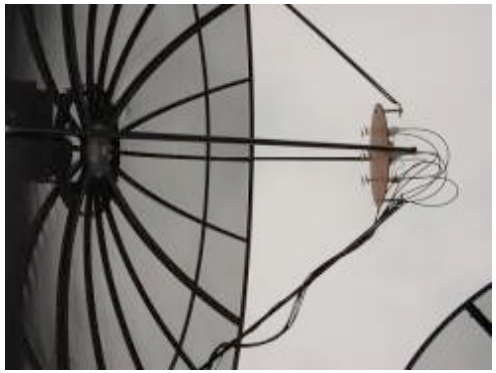

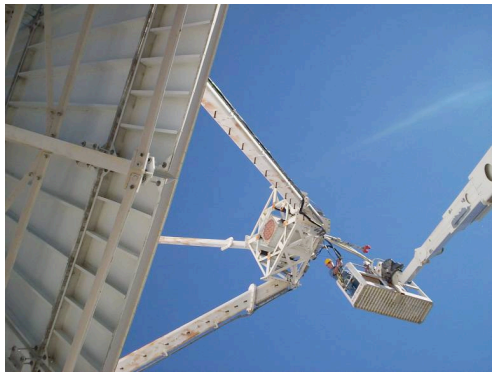

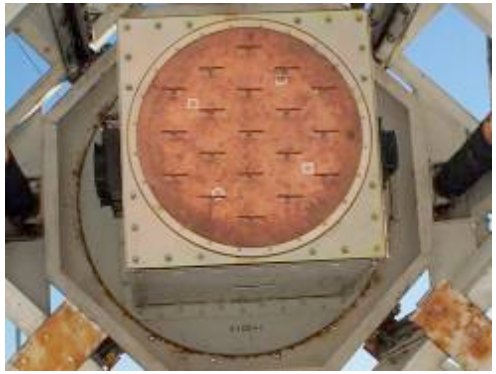

PAF analysis and modeling

System performance metrics are proposed and detailed analytical models are developed

System Model

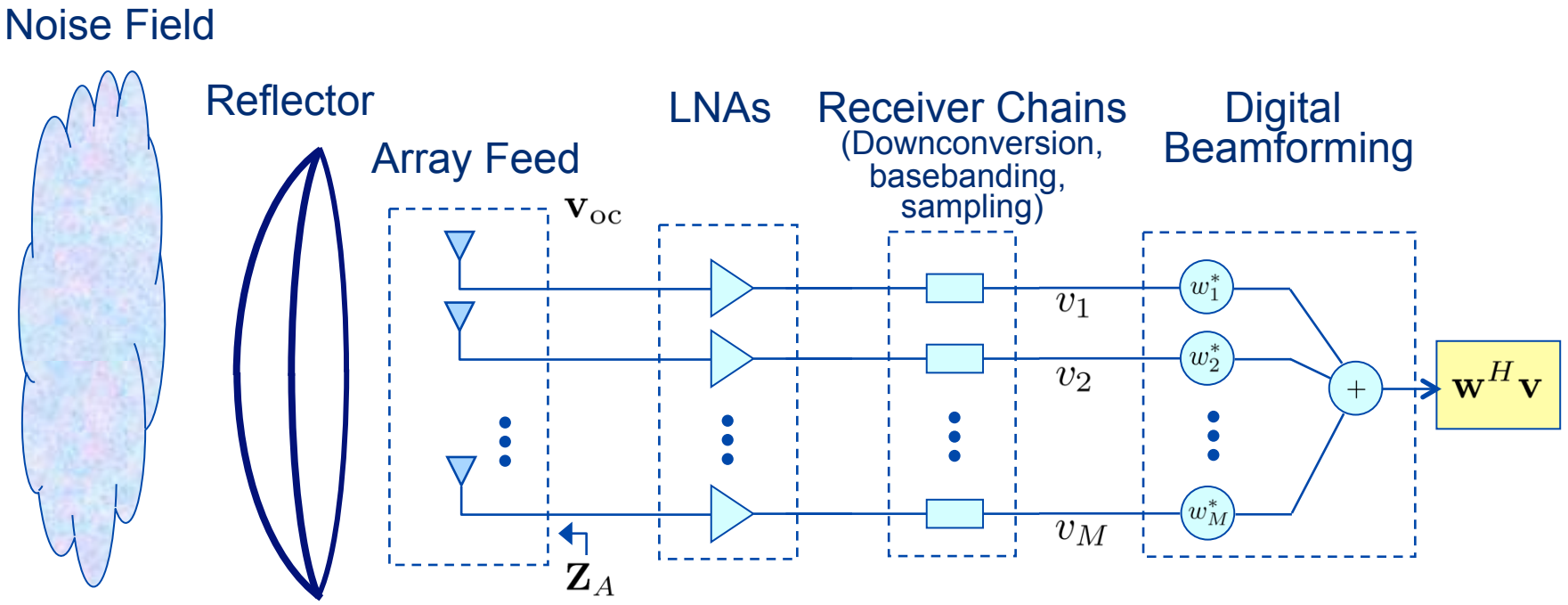

Dense grid for ground and sky

Physical Optics

Full wave EM simulation (Ansoft HFSS)

Network Theory

Signal, noise correlation matrices

Array Signal Processing

Candidate Beamforming Modes

- **Fixed beams:** (RF/analog), precalibrated, difficult to design.
- **Phase only beam steering**, precalibrated.
- **"Fixed-adaptive" beamforming:**
  - [Jeffs & Warnick, 2007]
  - Calibrate beams using strong point source on steering grid.
  - Optimize sensitivity/SNR for a given pointing direction using maximum SNR beamforming algorithm:

$$\mathbf{R}_{\text{sig}}\mathbf{w} = \lambda_{\max}\mathbf{R}_{\text{noise}}\mathbf{w}$$

  - Periodic adaptation (recalibration) on order of a few days.
- **Slow adaptation:** Irregular updates to noise field changes due to elevation steering. (order of minutes).
- **Fast adaptation:** (Periodic adaptation on order of milliseconds).
  - RFI mitigation: subspace projection, max-SINR algorithms.
  - "Pattern rumble" must be overcome for high sensitivity radiometry.

Array Calibration

- 31×31 raster grid of reflector pointing directions:
  - Centered on calibrator source
    Cas A, Tau A, Virgo A, GOES satellite.
  - 10 sec integration time per pointing.
  - Acquire array covariance matrices $\mathbf{R}_{\mathrm{sig},j}$.
- One off-pointing per cross elevation row to estimate $\mathbf{R}_{\mathrm{noise}}$ (2-5 degrees away).
- Beamformer weight vector for the jth pointing is obtained by solving the generalized eigenvalue problem

$$(\mathbf{R}_{\mathrm{on},j} - \mathbf{R}_{\mathrm{off}})\mathbf{w} = \lambda_{\max}\mathbf{R}_{\mathrm{off}}\mathbf{w}$$

- Calibrations stable for days.

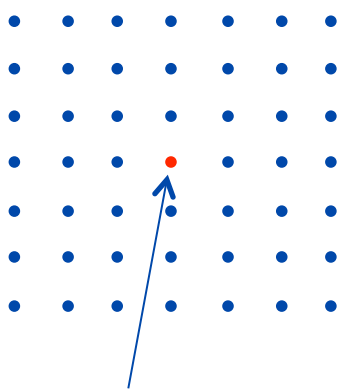

Array output voltage correlation matrix: $\mathbf{R}_{\mathrm{on}} = \mathrm{E}[\mathbf{v}\mathbf{v}^H] = \mathbf{R}_{\mathrm{sig}} + \underbrace{\mathbf{R}_{\mathrm{sp}} + \mathbf{R}_{\mathrm{rec}} + \mathbf{R}_{\mathrm{sky}} + \mathbf{R}_{\mathrm{loss}}}_{\mathbf{R}_{\mathrm{noise}} = \mathbf{R}_{\mathrm{off}}}$

Array Characterization

- Aperture efficiency and system temperature cannot be extracted without additional measurements
- How can the directivity of an active receiving array be measured?
  - No single port to which available power can be referred
  - Different gains in each signal path
  - Directivity cannot be determined from a single signal power measurement
  - Integrated pattern required for normalization
- Range measurements are difficult:
  - Requires full sphere element receiving patterns or full sphere beam receiving pattern
  - Characterization of the array as a transmitter requires element by element measurement and patterns must be embedded into receiver system
- *Is there a better measurement technique?*

Beam Sensitivity and Efficiencies

Sensitivity:

$$\frac{A_\mathrm{e}}{T_\mathrm{sys}} = \frac{k_b B}{S^\mathrm{sig}} \mathrm{SNR} \quad (\mathrm{m}^2/\mathrm{K})$$

$$\frac{A_\mathrm{e}}{T_\mathrm{sys}} = \frac{2k_\mathrm{b}}{10^{-26} F^\mathrm{sig}} \frac{\mathbf{w}^H \mathbf{R}_\mathrm{on} \mathbf{w} - \mathbf{w}^H \mathbf{R}_\mathrm{off} \mathbf{w}}{\mathbf{w}^H \mathbf{R}_\mathrm{off} \mathbf{w}} \quad \longleftarrow P_\mathrm{sig} \quad \longleftarrow P_\mathrm{noise}$$

$$= \frac{\eta_\mathrm{rad} \eta_\mathrm{ap} A_\mathrm{p}}{T_\mathrm{sky} + \underbrace{\eta_\mathrm{rad}(1-\eta_\mathrm{sp})T_\mathrm{g}}_{T_\mathrm{sp}} + \underbrace{(1-\eta_\mathrm{rad})T_a}_{T_\mathrm{loss}} + \underbrace{T_\mathrm{min}/\eta_\mathrm{n}}_{T_\mathrm{rec}}}$$

Efficiencies:

Aperture efficiency: $\eta_\mathrm{ap} = \frac{k_b T_\mathrm{iso}}{A_p (F^\mathrm{sig}/2)} \frac{\mathbf{w}^H \mathbf{R}_\mathrm{sig} \mathbf{w}}{\mathbf{w}^H \mathbf{R}_\mathrm{iso} \mathbf{w}}$

Spillover efficiency: $\eta_\mathrm{sp} = 1 - \frac{\mathbf{w}^H \mathbf{R}_\mathrm{sp} \mathbf{w}}{\mathbf{w}^H \mathbf{R}_\mathrm{iso} \mathbf{w}}$

Noise correlation for perfect "sky"

Radiation efficiency: $\eta_\mathrm{rad} = \frac{\mathbf{w}^H \mathbf{R}_\mathrm{iso} \mathbf{w}}{\mathbf{w}^H (\mathbf{R}_\mathrm{iso} + \mathbf{R}_\mathrm{loss}) \mathbf{w}}$

Noise matching efficiency: $\eta_\mathrm{n} = \frac{T_\mathrm{min}}{T_\mathrm{iso}} \frac{\mathbf{w}^H \mathbf{R}_\mathrm{iso} \mathbf{w}}{\mathbf{w}^H \mathbf{R}_\mathrm{rec} \mathbf{w}}$

Consistent with IEEE Standard Definition of Terms for Antennas

Warnick and Jeffs, "Efficiencies and system temperature for a beamforming array," AWPL, 2008]

Cold Sky/Warm Absorber Setup

Array Y Factor Measurement

Absorber: $\mathbf{R}_{\rm hot} = \frac{T_{\rm hot}}{T_{\rm iso}}\mathbf{R}_{\rm iso} + \mathbf{R}_{\rm rec} + \mathbf{R}_{\rm loss}$

Sky: $\mathbf{R}_{\rm cold} = \frac{T_{\rm cold}}{T_{\rm iso}}\mathbf{R}_{\rm iso} + \mathbf{R}_{\rm rec} + \mathbf{R}_{\rm loss}$

$$\mathbf{R}_{\rm iso} = \frac{T_{\rm iso}}{T_{\rm hot} + T_{\rm cold}}(\mathbf{R}_{\rm hot} - \mathbf{R}_{\rm cold})$$

$$\mathbf{R}_{\rm rec} + \mathbf{R}_{\rm loss} = \frac{T_{\rm hot}\mathbf{R}_{\rm cold} - T_{\rm cold}\mathbf{R}_{\rm hot}}{T_{\rm hot} - T_{\rm cold}}$$

Isotropic noise response allows efficiency and system temperature to be determined from on/off source pointings:

$$\eta_{\rm ap} = \frac{k_b T_{\rm iso} B}{A_p S^{\rm sig}} \frac{\mathbf{w}^H \mathbf{R}_{\rm sig} \mathbf{w}}{\mathbf{w}^H \mathbf{R}_{\rm iso} \mathbf{w}}$$

$$T_{\rm sys}/\eta_{\rm rad} = T_{\rm iso} \frac{\mathbf{w}^H \mathbf{R}_{\rm noise} \mathbf{w}}{\mathbf{w}^H \mathbf{R}_{\rm iso} \mathbf{w}}$$

On-Reflector Results (July 2008)

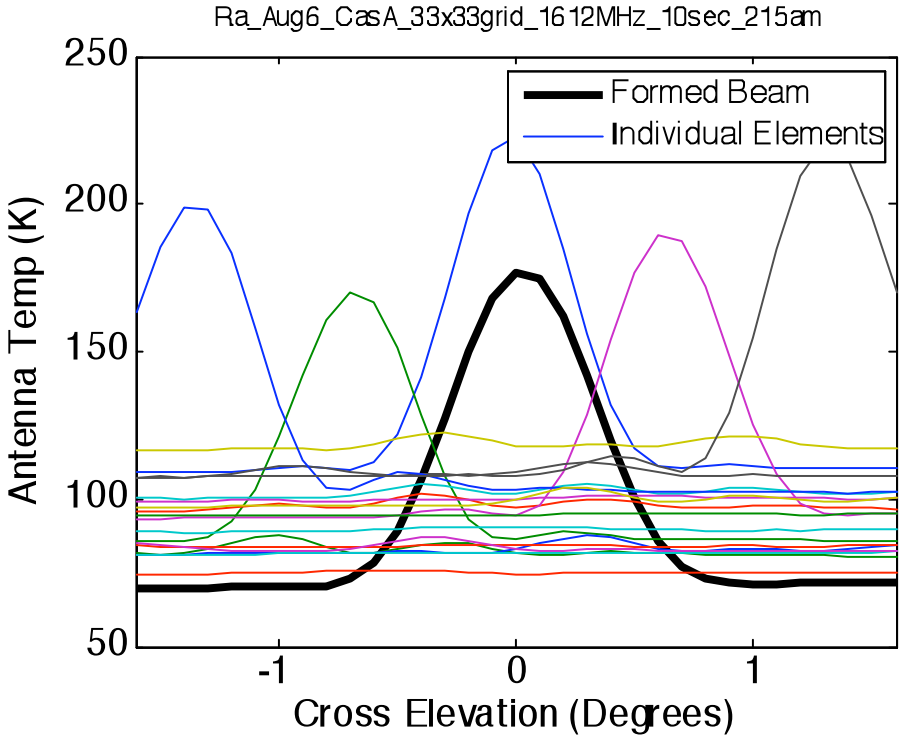

Cas A scan
1612 MHz

	Center Element	**Formed Beam**	Model (FEM)
Sensitivity:	2 m^2/K	**3.3 m^2/K**	3.7 m^2/K
T_{sys}:	101 K	**66 K**	69 K
Efficiency:	64%	**69%**	81%

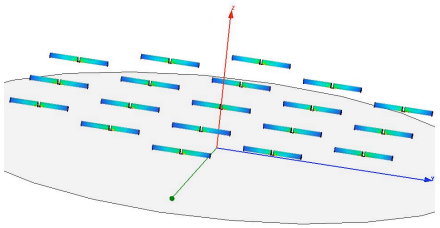

System Noise Budget

	Measured	Model	
LNA T_{min}	33 K	33 K	
Mutual coupling	20 K	23 K	← Noise matching efficiency 60%
Spillover	5 K	5 K	
Sky	3 K	3 K	
Loss	5 K	5 K	
T_{sys}:	**66 K**	**69 K**	

Mutual Coupling Noise Penalty

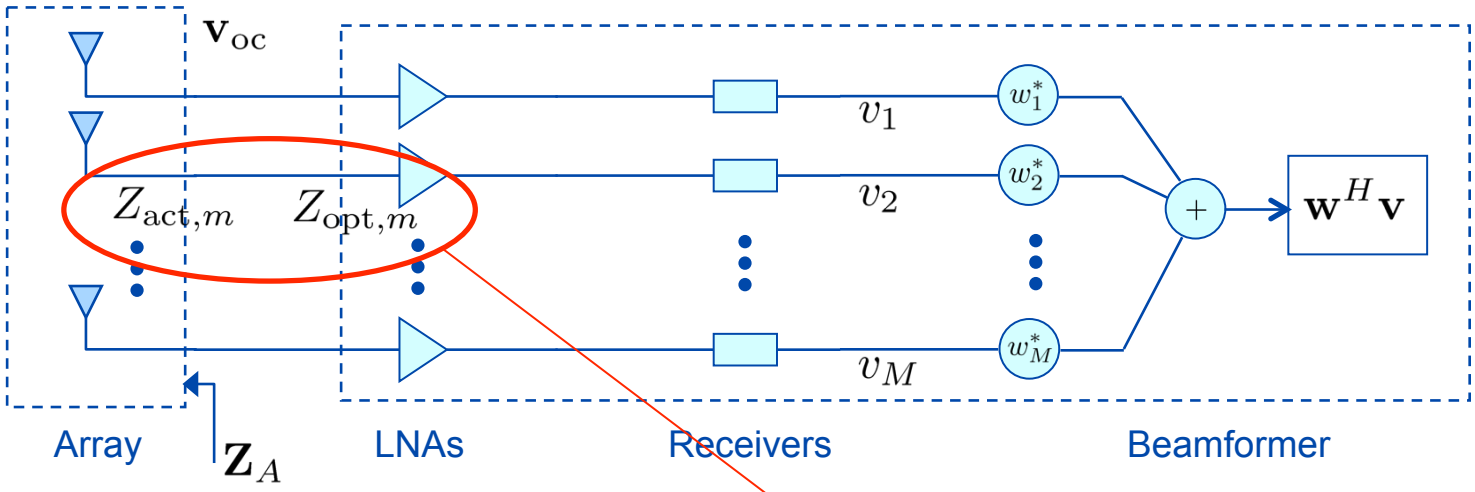

Active impedances [Woestenburg, 2005]:

$$Z_{\mathrm{act},m} = \frac{1}{w_{\mathrm{oc},m}^*} \sum_{n=1}^{M} w_{\mathrm{oc},n}^* Z_{A,nm}$$

$$T_{\mathrm{rec}} = T_{\mathrm{min}} + T_0 \frac{\sum_{m=1}^{M} |w_{\mathrm{oc},m}|^2 R_{n,m} |Z_{\mathrm{act},m}|^2 |Y_{\mathrm{act},m} - Y_{\mathrm{opt},m}|^2}{\sum_{m=1}^{M} |w_{\mathrm{oc},m}|^2 R_{\mathrm{act},m}}$$

$Z_{\mathrm{act},m} \neq 50\,\Omega \Rightarrow$ *20 K increase in effective LNA noise*

Noise Matching

Isolated impedance match

Poor performance for embedded elements

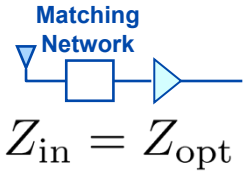

$$Z_{\text{in}} = Z_{\text{opt}}$$

Self impedance match

Performance still poor

$$Z_{\text{A},mm} = Z_{\text{opt},m}$$

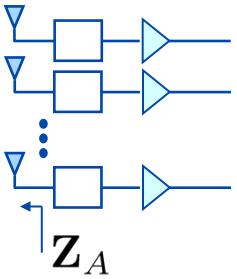

Active impedance match (beam dependent)

Only maximizes SNR for one beam

Unstable for PAFs

$$Z_{\text{opt},m} = \frac{1}{w^*_{\text{oc},m}} \sum_{n=1}^{M} w^*_{\text{oc},n} Z_{A,nm}$$

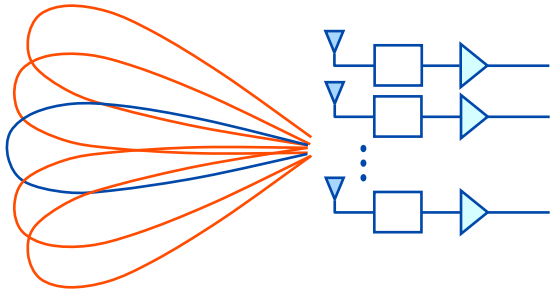

Decoupling network

Optimal for all beams

Lossy, narrowband

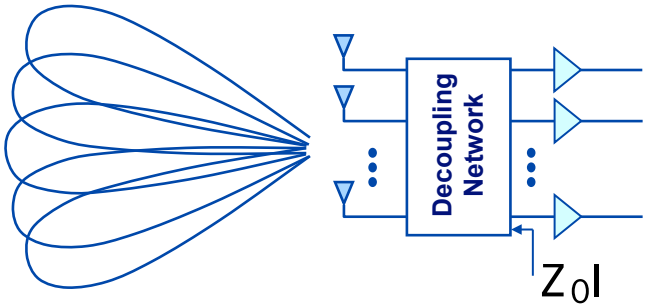

Field of View Optimal Matching

- LNA optimal impedance parameter:

$$Z_{\mathrm{opt},m} = \frac{\sum_{p=1}^{P} |w_{\mathrm{oc},m}^{p}|^2 |Z_{\mathrm{act},m}^{p}|^2}{\sum_{p=1}^{P} |w_{\mathrm{oc},m}^{p}|^2 Z_{\mathrm{act},m}^{p\,*}}$$

- Minimizes average noise over *P* beams that span the array field of view
- Leads to stable impedances
- If the field of view is a full sphere:

$$Z_{\mathrm{opt},m} = \frac{[\mathbf{Z}_A^H \mathrm{Re}[\mathbf{Z}_A]\mathbf{Z}_A]_{mm}}{[\mathrm{Re}[\mathbf{Z}_A]\mathbf{Z}_A]_{mm}^*}$$

[Warnick, Woestenburg, Belostotski, and Russer, TAP, 2009]

Radio camera results

Demonstration of PAF image mosaicing on the
Green Bank 20 meter Telescope, July 2008

Element Patterns

Source: Cas A, 1612 MHz
0.1 degree pointing grid

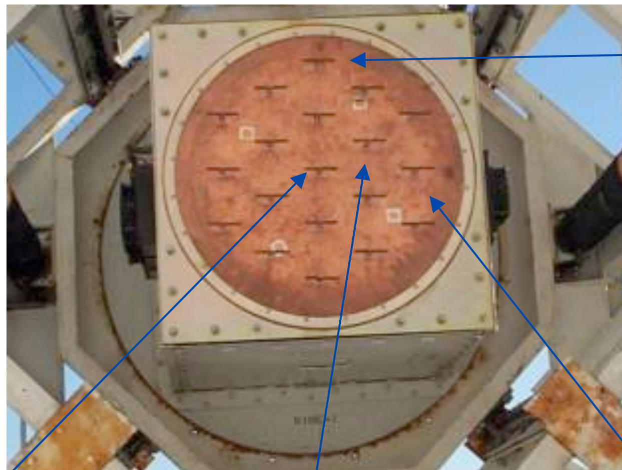

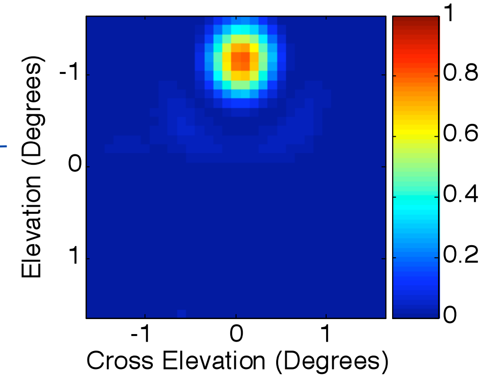

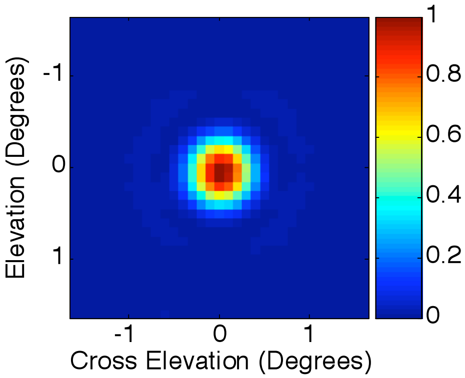

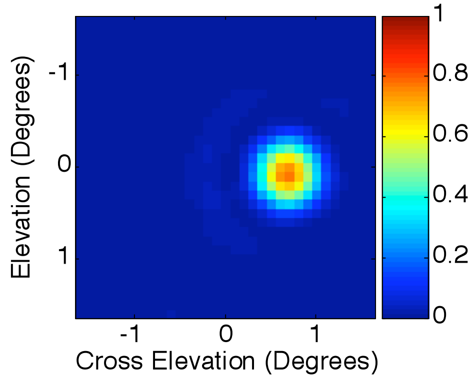

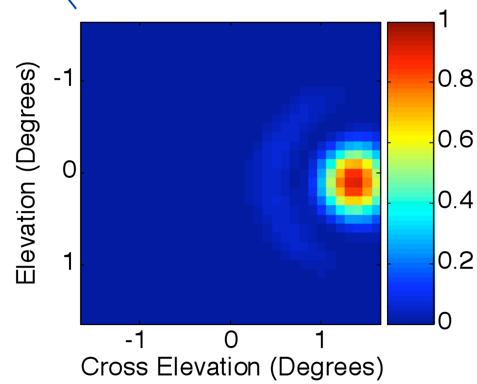

Scale: Linear relative to center element max

Beam Patterns

Boresight

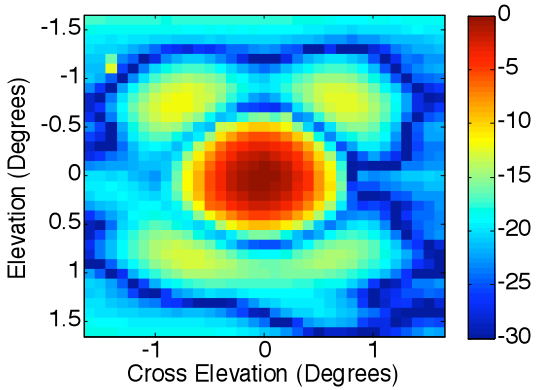

0.4º

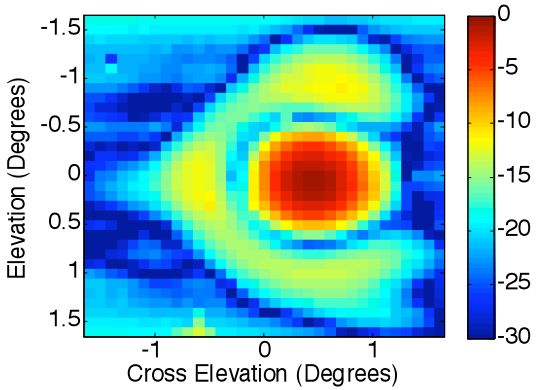

0.8º

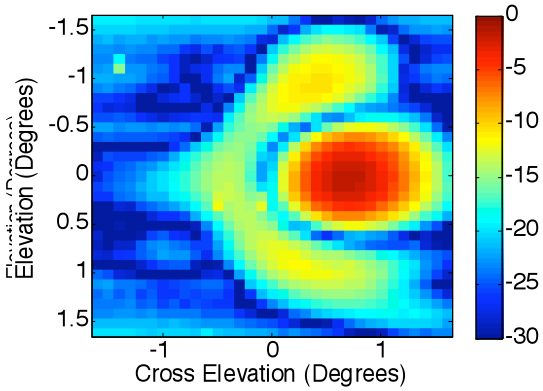

1.2º

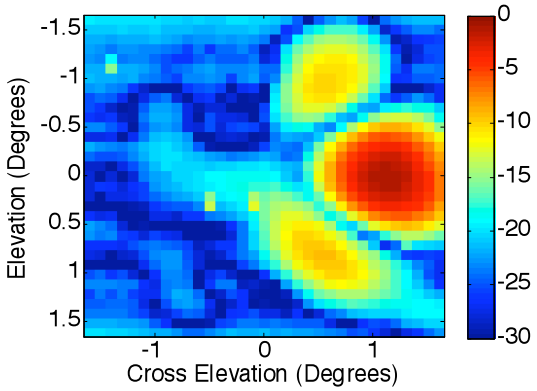

Scale: dB relative to boresight beam max

Beam Sensitivity, Efficiency, T_{sys}

Beam Sensitivity (m^2/K)

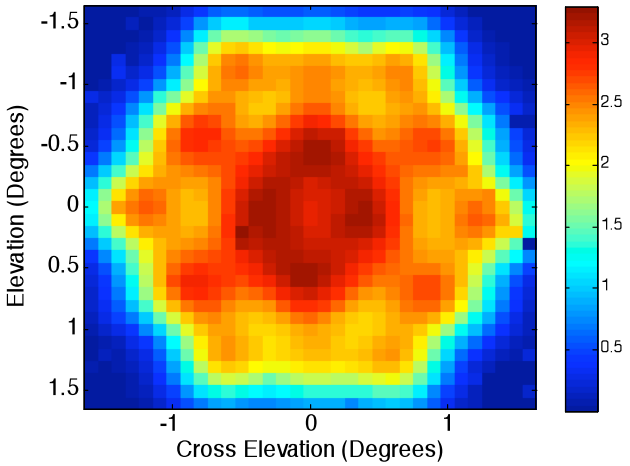

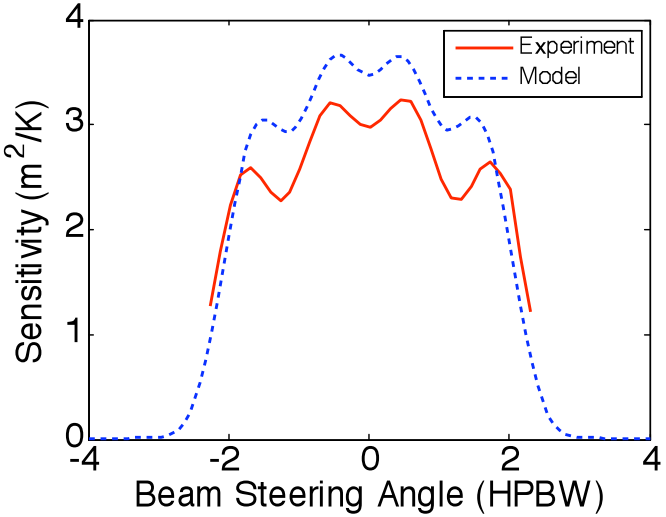

FOV ~ ±1°
Defined by 1dB sensitivity loss

Beam Aperture Efficiency

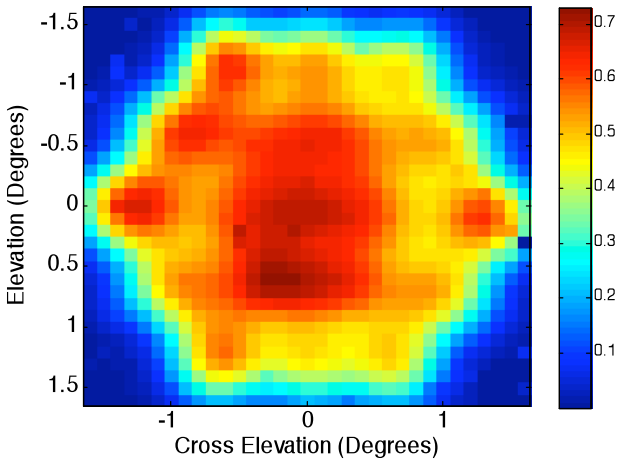

Beam T_{sys}

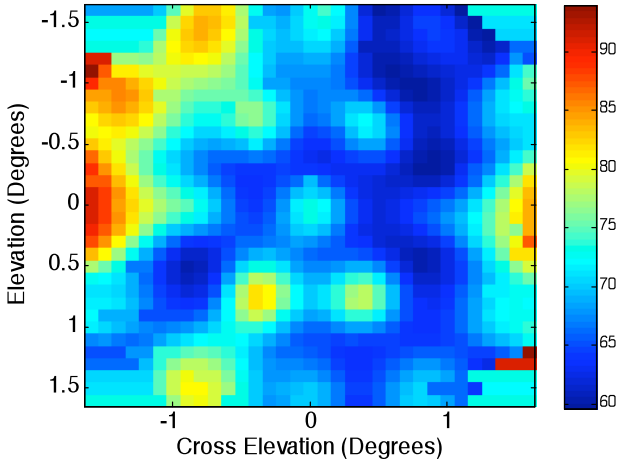

Single Pointing Image - 3C295

Source: 3C295
Flux density: 21 Jy at 1400 MHz
Observation freq. 1612 MHz
Integration time: 60 sec

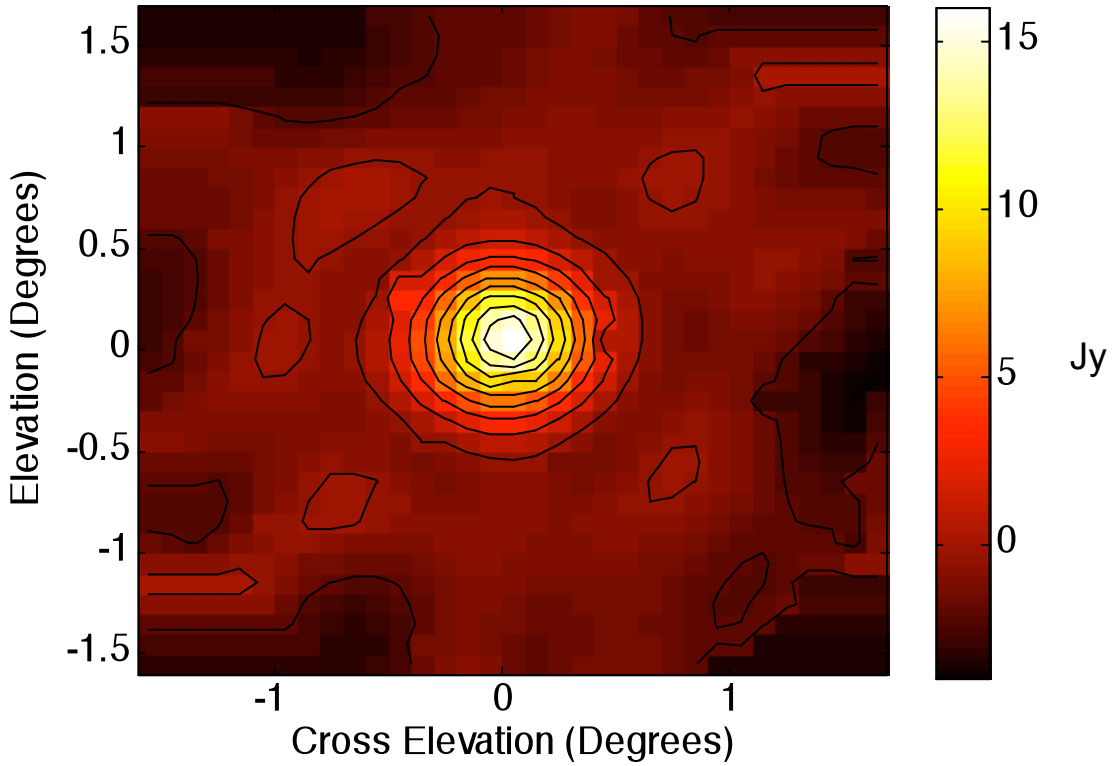

Adaptive RFI Mitigation

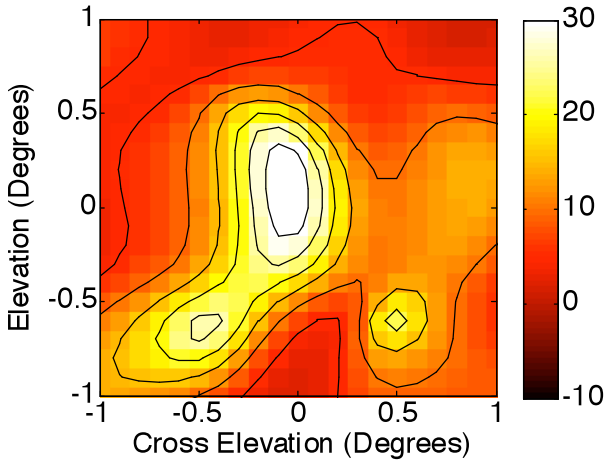

W3OH, no RFI

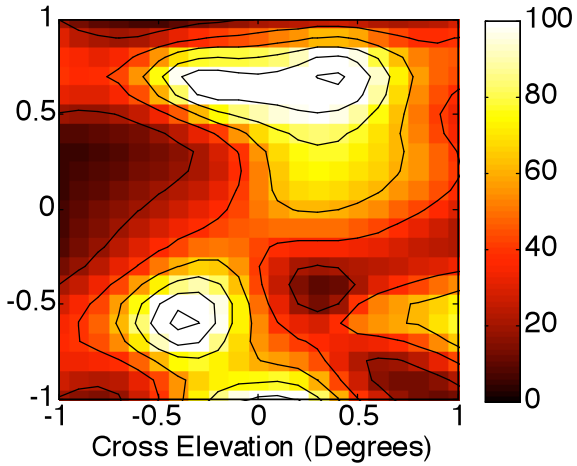

RFI corrupted image
(moving function generator
and antenna on the ground)

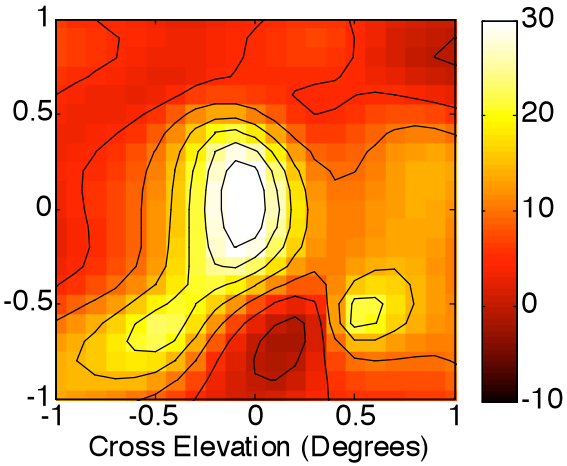

Adaptive spatial filtering
Subspace projection algorithm

Cygnus X Region at 1600 MHz

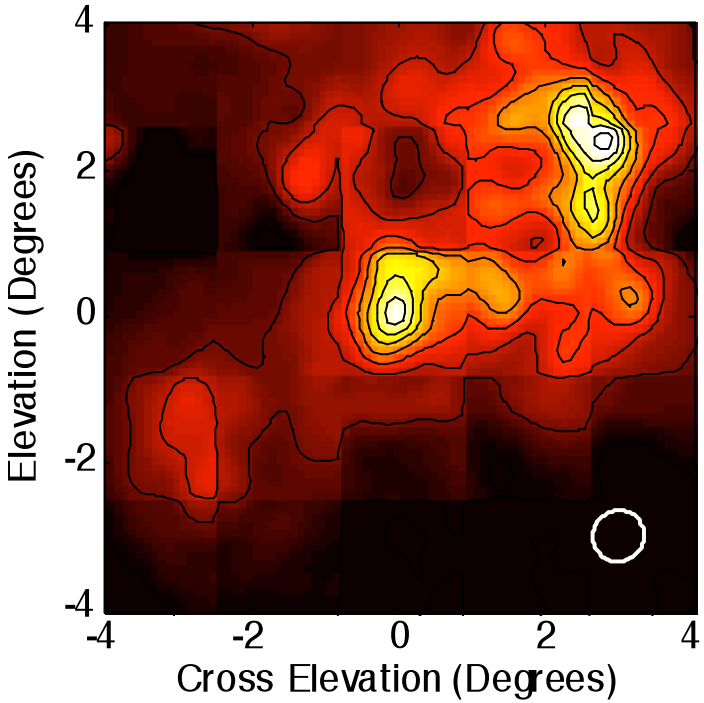

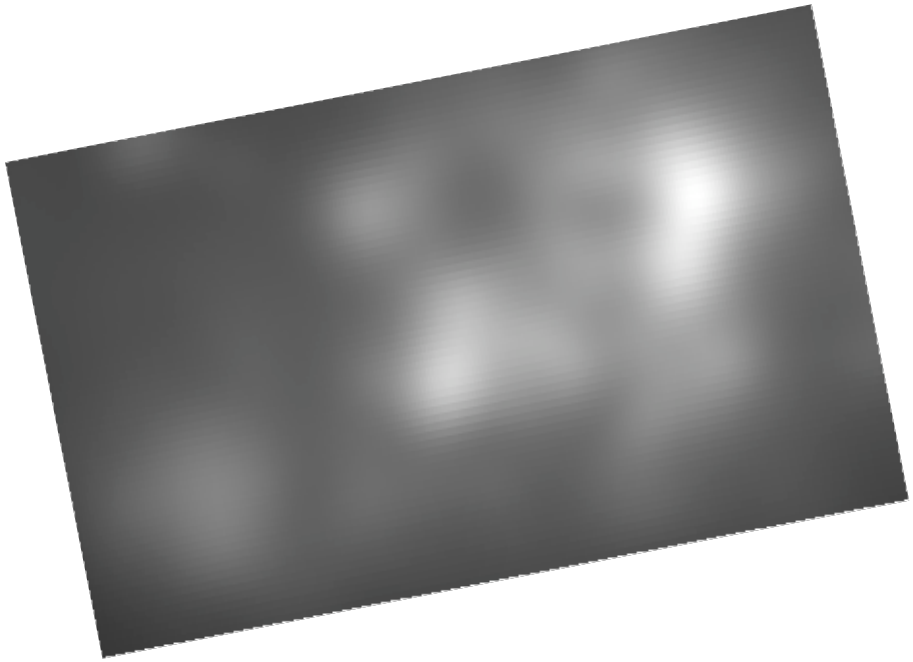

5 x 5 mosaic of PAF pointings
Circle indicates half power beamwidth
Required antenna pointings:

- Single-pixel feed: ~600
- PAF: 25
- **Imaging speedup: 24x**

Canadian Galactic Plane Survey
Convolved to 20-Meter beamwidth

Image Mosaic - W49 Region

1612 MHz
3 x 3 = 9 pointings

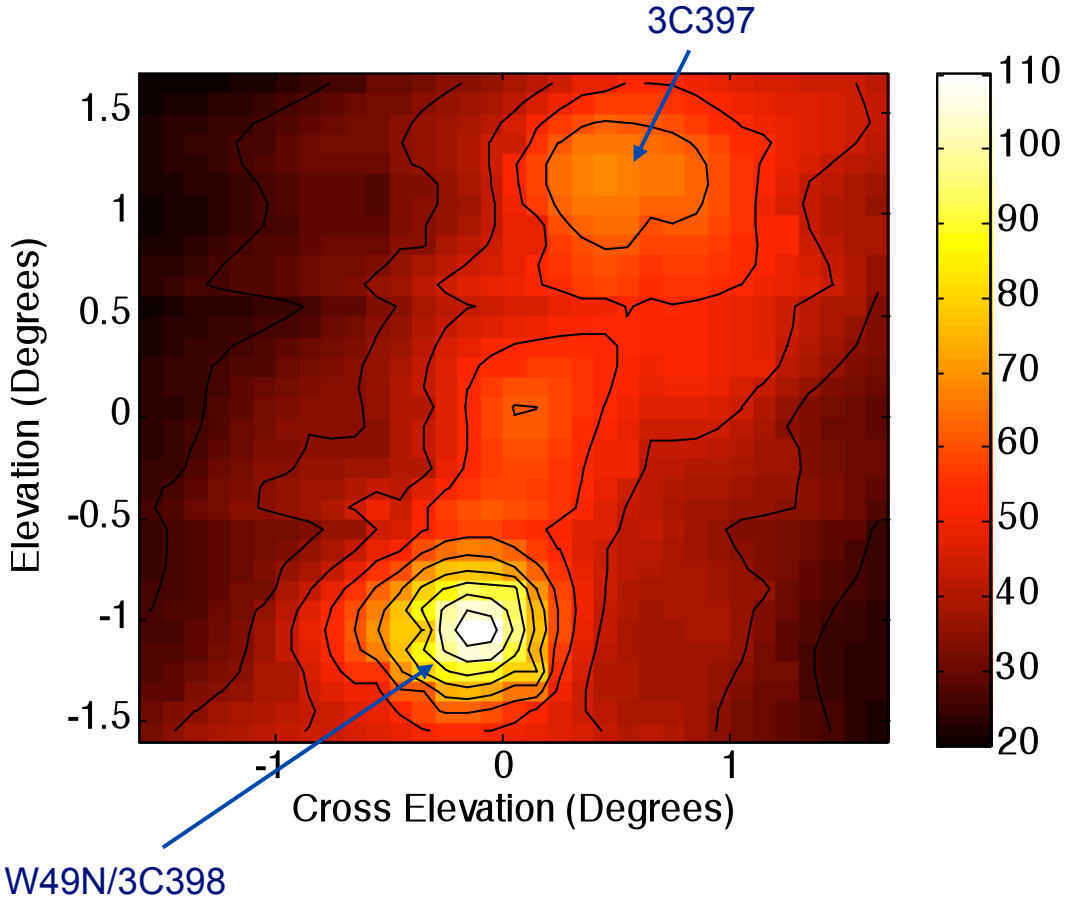

Sensitivity optimization to elevation dependent noise

Demonstrating the performance potential
for an adaptive PAF

Elevation Dependent Noise Covariance

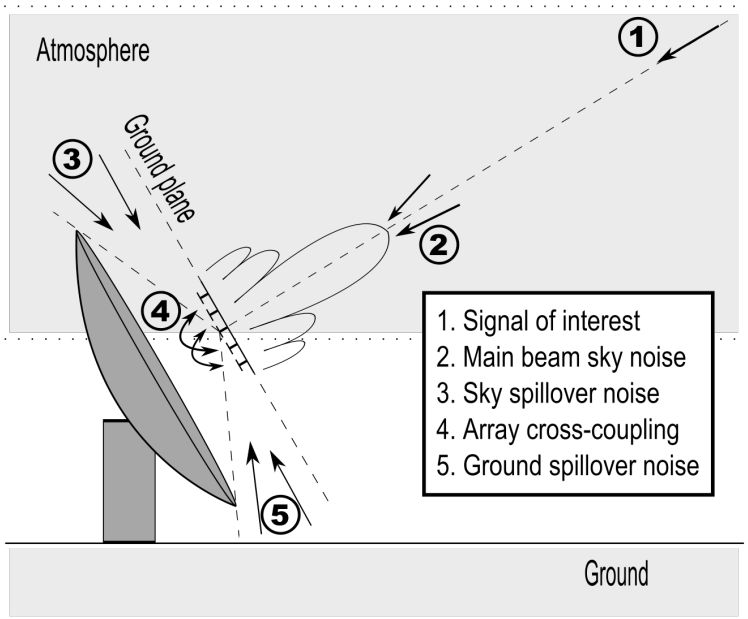

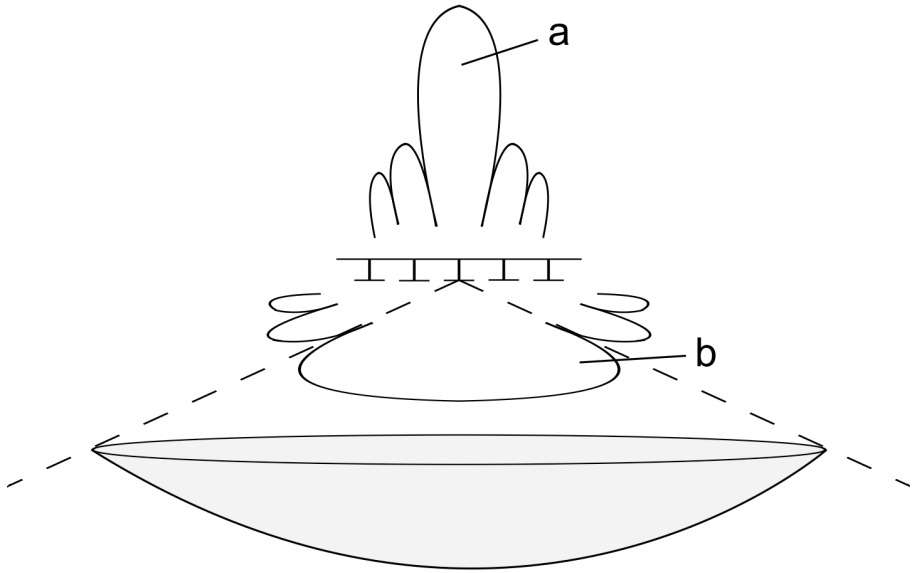

Spillover region is numerically modeled as a grid of point sources. As the dish is tipped, a portion of the spillover region passes through the sky/ground plane and sees the colder sky.

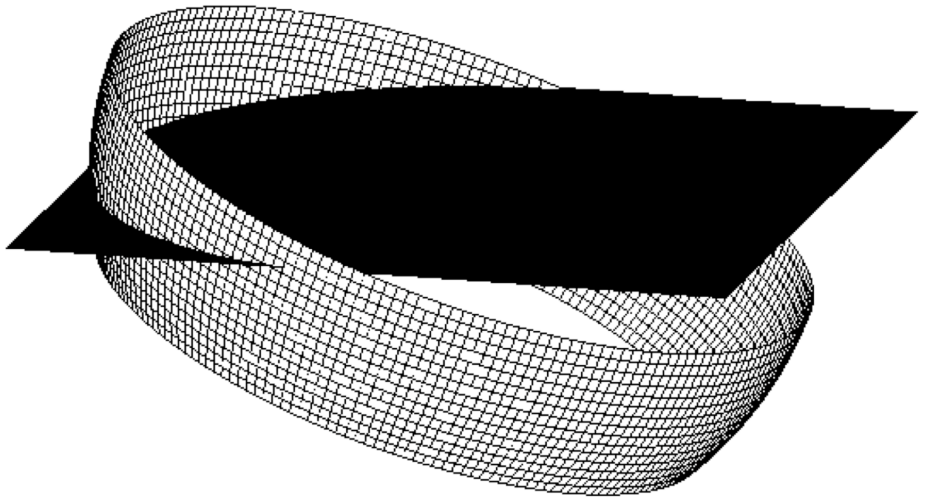

Spillover and Sky Noise Models

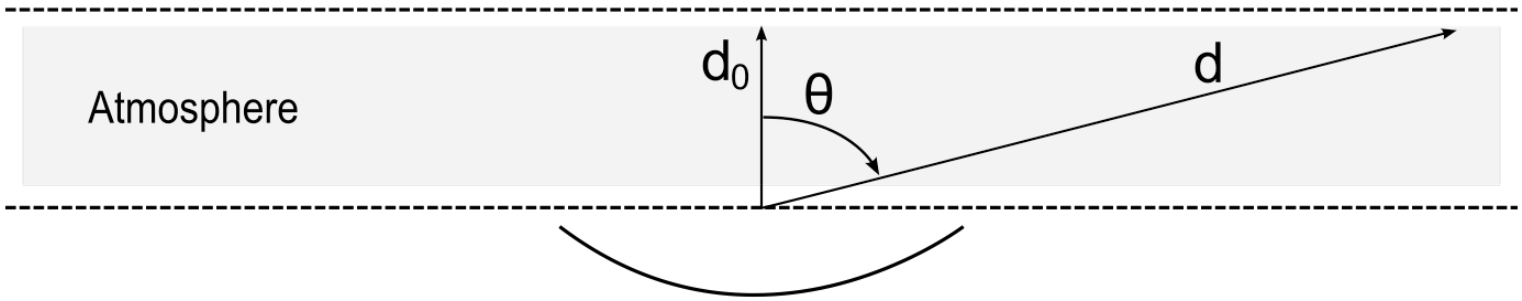

- Main beam sky noise model:

$$\mathbf{R}_{\text{mb}} = T_{\text{mb}}\mathbf{A}_{\text{iso}}, \qquad T_{\text{mb}}(\theta) = T_0 \sec(80^\circ) + 1.3(\theta - 80^\circ), \quad T_0 = 2K$$

- Discrete spillover noise model:

$$\mathbf{R}_{\text{SP}} = \frac{16k_bB}{|I_0|^2}\frac{1}{2\eta}\sum_p T_p \mathbf{a}_p \mathbf{a}_p^H A_p, \quad T_p = \begin{cases} 293K & \text{below horizon} \\ T_{\text{mb}}(\theta_p) & \text{above horizon} \end{cases}$$

where $\mathbf{a}_p$ is the array response vector to the pth noise point location and A_p is the area covered by that grid point

- Total noise model:

$$\mathbf{R}_{\text{noise}} = \mathbf{R}_{\text{rec}} + \mathbf{R}_{\text{sp}} + \mathbf{R}_{\text{mb}}, \qquad T_{\text{sys}} = T_{\text{iso}}\frac{\mathbf{w}^H\mathbf{R}_{\text{noise}}\mathbf{w}}{\mathbf{w}^H\mathbf{R}_{\text{iso}}\mathbf{w}}$$

Simulation Results

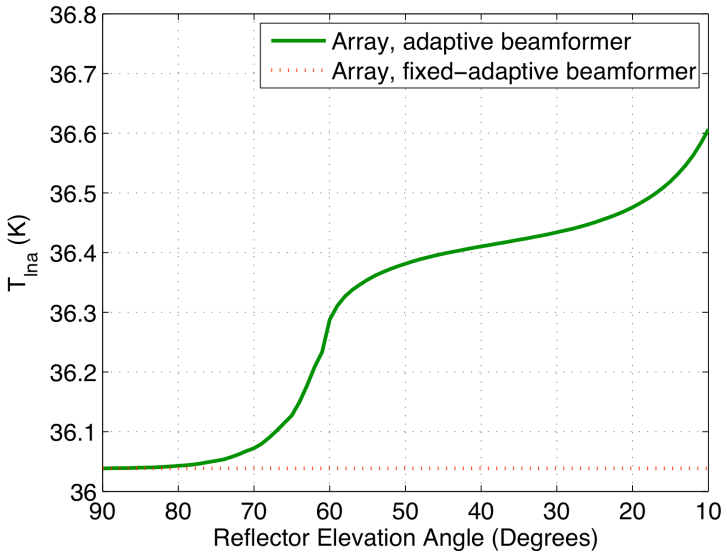

Receiver noise

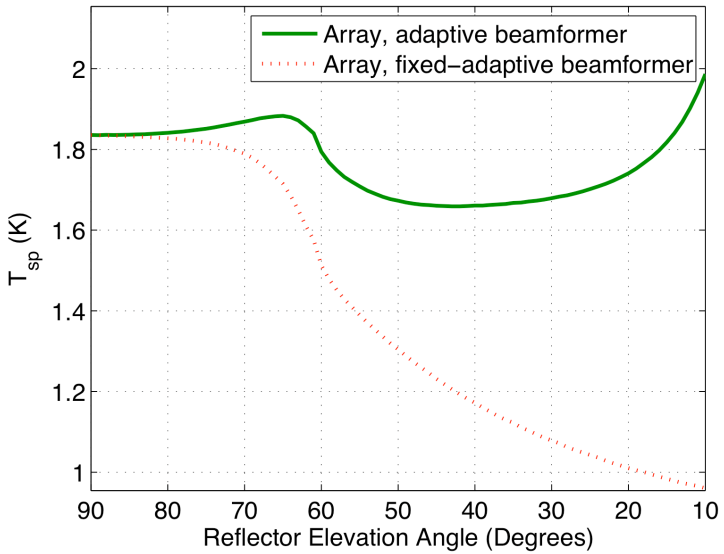

Spillover noise

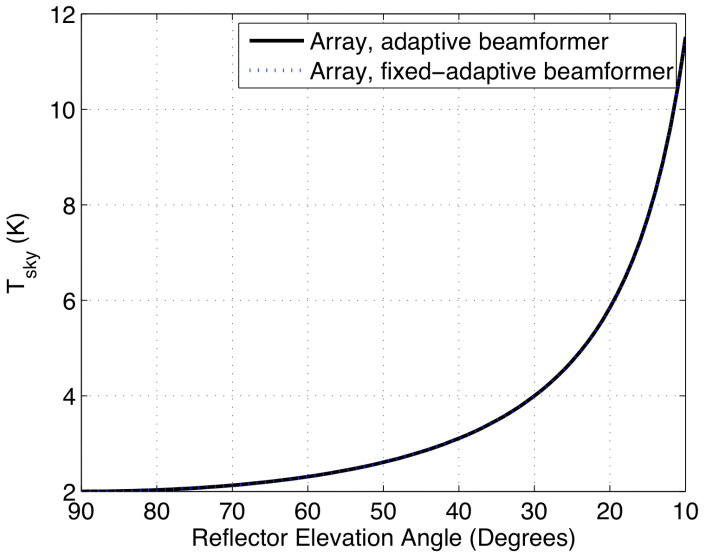

main beam sky noise

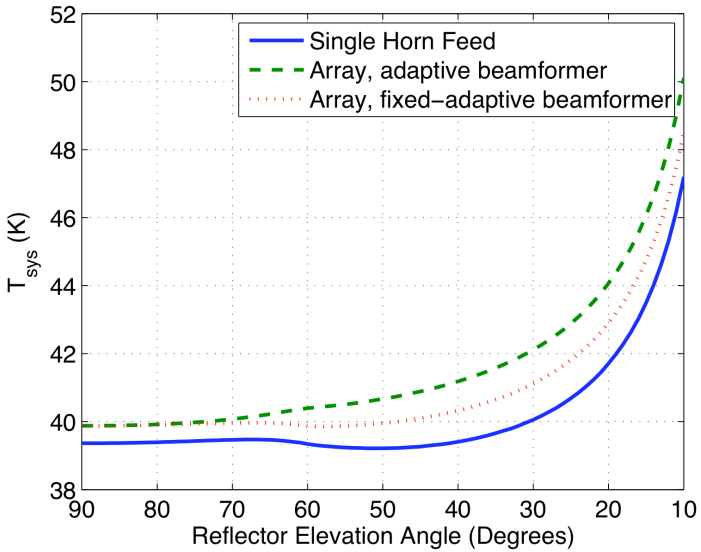

System noise

Simulation Results (2)

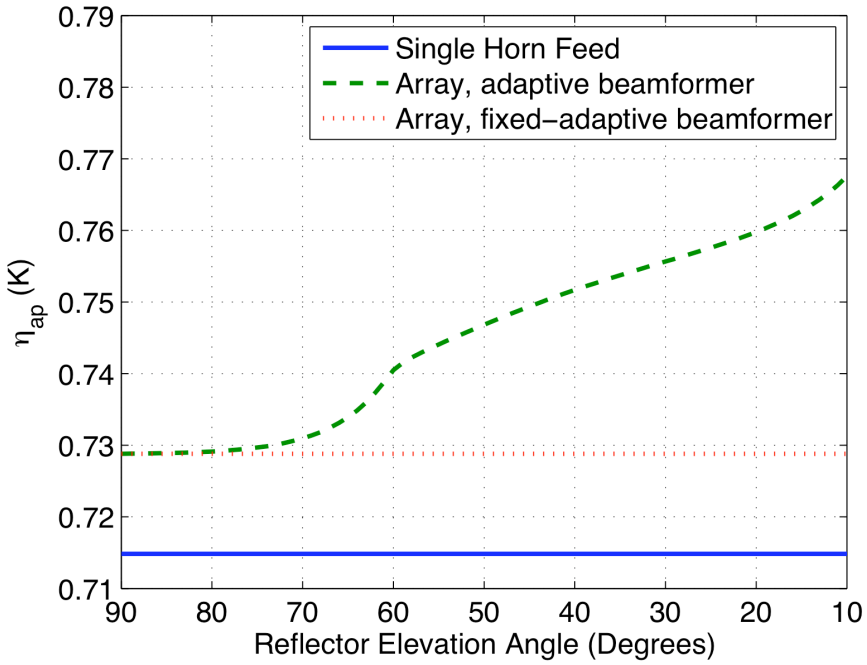

Aperture Efficiency

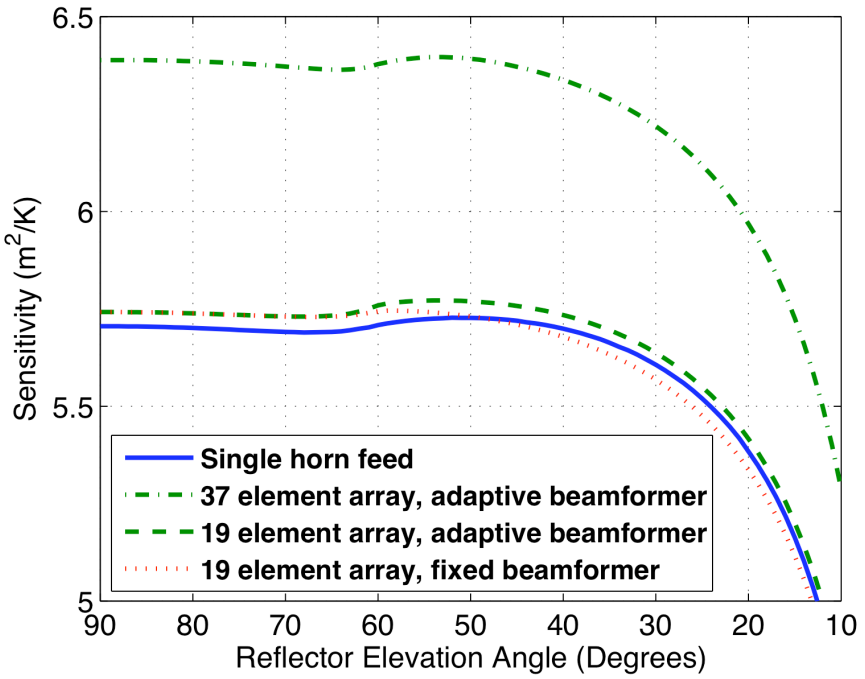

System Sensitivity

20m dish Real Data Comparisons

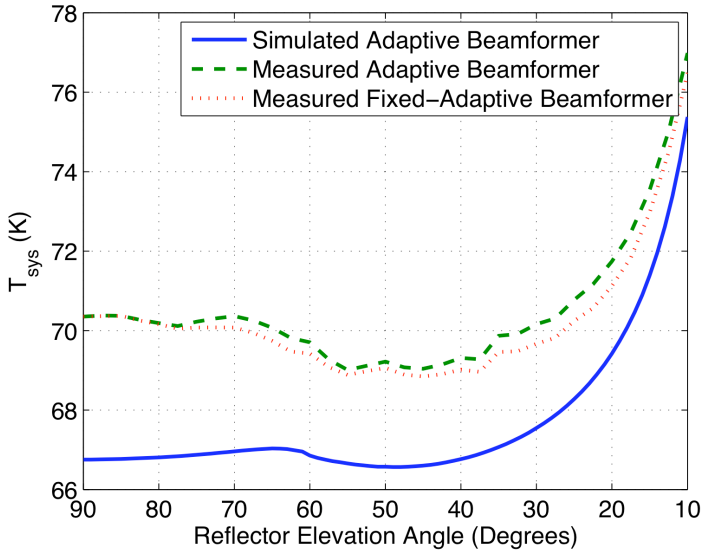

System Temperature

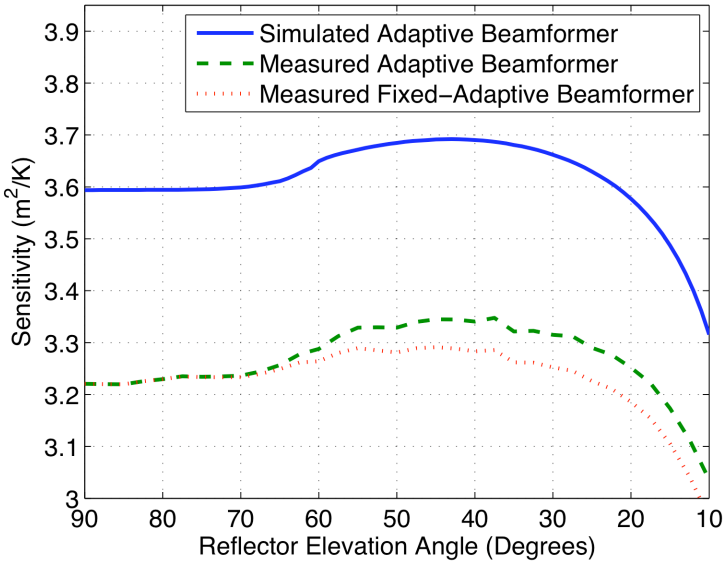

System Sensitivity

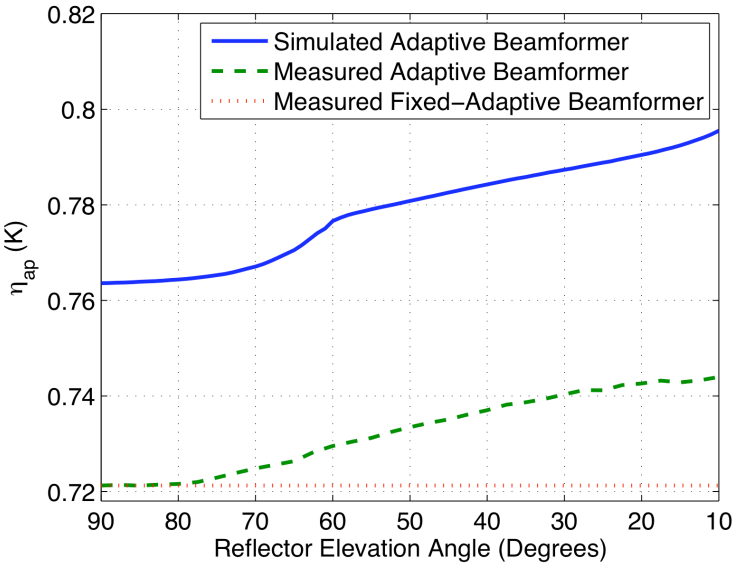

Aperture Efficiency

Deep Null Adaptive Interference Canceling for Phased Array Feeds

Polynomial model-based method provides better performance for low INR cases.

Challenges for Astronomical Adaptive Array RFI Canceling

- Beampattern nulls must be deep to drive an interferer *well* below the noise floor to reveal the SOI.
- Low INR interferers are hard to cancel, can't accurately estimate interference parameters.
- Conventional block update cancellation null depth is limited by:
  - Sample estimation error in $\hat{\mathbf{R}}_{\text{int},k}$.
  - Subspace smearing due to motion within a short-time integration (STI) window.
  - Subspace Partitioning errors (signal-noise-interference overlap, bias).
  - Methods do not exploit knowledge that interferer motion is smooth, continuous.
  - Short STIs avoid motion cause subspace smearing in $\hat{\mathbf{R}}_k = \hat{\mathbf{R}}_{\text{sig},k} + \hat{\mathbf{R}}_{\text{noise},k} + \hat{\mathbf{R}}_{\text{int},k}$.
  - But, short STIs increase sample estimation error.
- Solution:
  - Fit interference $\hat{\mathbf{R}}_{\text{int},k}$ to a matrix polynomial model over many STIs.
  - Decrease both sample estimation error and subspace smearing.
  - Better estimates of $\hat{\mathbf{R}}_{\text{int},k}$ yield deeper cancellation nulls!

Conventional Subspace Projection (SSP)

- This zero-forcing method can place deeper nulls than max SNR, LCMV, MVDR, Weiner filter, and other array cancellers
- At *k*th STI, form an orthogonal projection matrix for the interferer(s):
  - Sample STI covariance estimate:

$$\hat{\mathbf{R}}_k = \frac{1}{N}\sum_{n=0}^{N-1}\mathbf{v}[n+kN]\mathbf{v}^H[n+kN] \quad \text{for } k\text{th STI of length } N$$

  - Partition eigenspace. Largest eigenvalues(s) correspond to interference.

$$\hat{\mathbf{R}}_k[\mathbf{U}_{\text{int}} \mid \mathbf{U}_{\text{sig+noise}}] = [\mathbf{U}_{\text{int}} \mid \mathbf{U}_{\text{sig+noise}}]\Lambda$$

  - Form projection matrix:

$$\mathbf{P}_k = \mathbf{I} - \mathbf{U}_{\text{int}}\mathbf{U}_{\text{int}}^H$$

- Compute weights and beamform:

$$\mathbf{w}_{\text{SSP},k} = \mathbf{P}_k\mathbf{w}_{\text{nominal}}, \quad y[n] = \mathbf{w}_{\text{SSP},k}^H\mathbf{v}[n], \quad k = \left\lfloor \frac{n}{N} \right\rfloor$$

Conventional SSP Simulation Results

- 7-element PAF on 20m reflector, 0.43f/D
- Correlated spillover noise, mutual coupling, modeled 33K Ciao Wireless LNAs.
- Measured array element radiation patterns.
- Physical Optics, full 2D integration over reflector.
- Moving point interferer
  - Average element INR: -5.01 dB.
  - Motions covers 20 – 21.8° AZ and 44 – 45.8° EL, 2.0° / sec.
  - Traverses 3 sidelobes of boresight beam.
- 291ksamp/sec, 0.9 seconds of data.

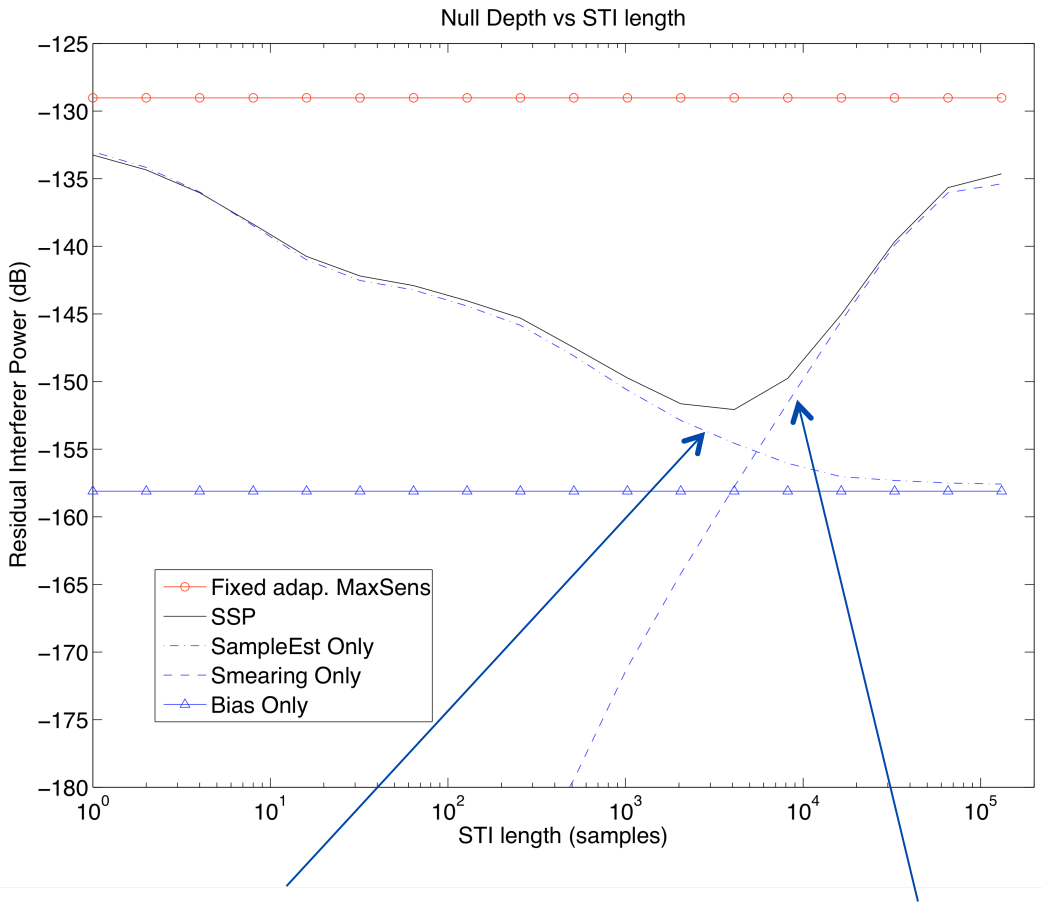

Subspace estimation error due to sample noise, i.e. null depth with no motion.

Subspace smearing error due to motion, i.e. null depth with no sample estimation error.

Low-order Parametric Model SSP

- Fit a series of STI covariances to a polynomial that can be evaluated at arbitrary timescale
  - Beamformer weights can be updated at every time sample, not just once per STI.
  - Use entire data window to fit polynomial ➔ less sample estimation error.
  - Exploit knowledge that physical motion yields smooth progression of $\mathbf{R}_{\text{int}}[n]$.

- Use a vector polynomial to model interference covariance at any time sample:

$$\mathbf{R}_{\text{int}}[n] \approx \tilde{\mathbf{R}}_{\text{int}}(t,\mathbf{C}) = \mathbf{a}_{\text{poly}}(t,\mathbf{C})\mathbf{a}_{\text{poly}}^{H}(t,\mathbf{C})\Big|_{t=nT_s}, \quad \text{where} \quad \mathbf{C} = [\mathbf{c}_0 \cdots \mathbf{c}_r],$$

$$\mathbf{a}_{\text{poly}}(t,\mathbf{C}) = \mathbf{c}_0 + \mathbf{c}_1 t + \cdots + \mathbf{c}_r t^r, \quad \text{and } T_s = \text{ sample period}$$

- Minimize the squared error between STI sample covariances and the polynomial model:

$$\mathbf{C}_{\text{LS}} = \arg\min_{\mathbf{C}} \sum_{k=1}^{K} \left\| \hat{\mathbf{R}}_k - \tilde{\mathbf{R}}_{\text{int}}(t_k,\mathbf{C}) \right\|_F^2, \quad \text{where} \quad t_k = kNT_s$$

Eigenvector Least Squares Fit (ELS)

- Find principal eigenvector for each STI

$$\hat{\mathbf{R}}_k \mathbf{u}_k = \lambda_{\max} \mathbf{u}_k$$

- Correct bulk phase ambiguity per STI by enforcing a smoothness constraint.
  - Phase shift each successive eigenvector so it is aligned as closely to the previous one as possible:

$$\alpha_k = \frac{\mathbf{u}_k^H \mathbf{u}_{k-1}}{\|\mathbf{u}_k\|^2} \qquad \mathbf{u}_{\text{smooth},k} = \frac{\alpha_k \mathbf{u}_k}{\|\alpha_k \mathbf{u}_k\|}$$

- Closed-form solution for polynomial coefficients

$$\mathbf{C}_{\text{ELS}} = (\mathbf{T}^T \mathbf{T})^{-1} \mathbf{T}^T \mathbf{U},$$

$$\mathbf{t} = [t_0 \cdots t_{K-1}]^T, \quad \mathbf{T} = [\mathbf{t}^r \ \mathbf{t}^{r-1} \cdots \mathbf{t}^0]$$

$$\mathbf{U} = [\mathbf{u}_0 \cdots \mathbf{u}_{K-1}]$$

Nonlinear Least Squares Fit (NLS)

$$\mathbf{C}_{\mathrm{NLS}} = \arg\min_{\mathbf{C}} \sum_{k=1}^{K} \left\| \hat{\mathbf{R}}_k - \tilde{\mathbf{R}}_{\mathrm{int}}(t_k, \mathbf{C}) \right\|_F^2, \quad \text{where } t_k = kNT_s$$

- Solve with MATLAB lsqnonlin function.
- $\mathbf{a}_{\mathrm{poly}}(t_k, \mathbf{C})$ is ambiguous over the STI sequence to within one phase term:
  - Must choose this term or the optimizer will not converge.
  - Arbitrarily set first element of zero order term $[\mathbf{c}_0]_1$ to be purely real.
- Use $\mathbf{C}_{\mathrm{ELS}}$ to initialize lsqnonlin and reduce convergence time.
- NLS is slower than ELS, but produces a better fit.

Polynomial-augmented SSP Results

- Polynomial order = 8.
- 13.4dB improvement over conventional SSP.
- EIG-SSP improves null depth by 11dB; NLS-SSP improves null depth by another 2.4dB.
- EIG-SSP requires enough averaging to get a good set of eigenvectors for regression.
- NLS-SSP computationally more difficult as STIs get shorter, but works over a wider range of STI lengths.

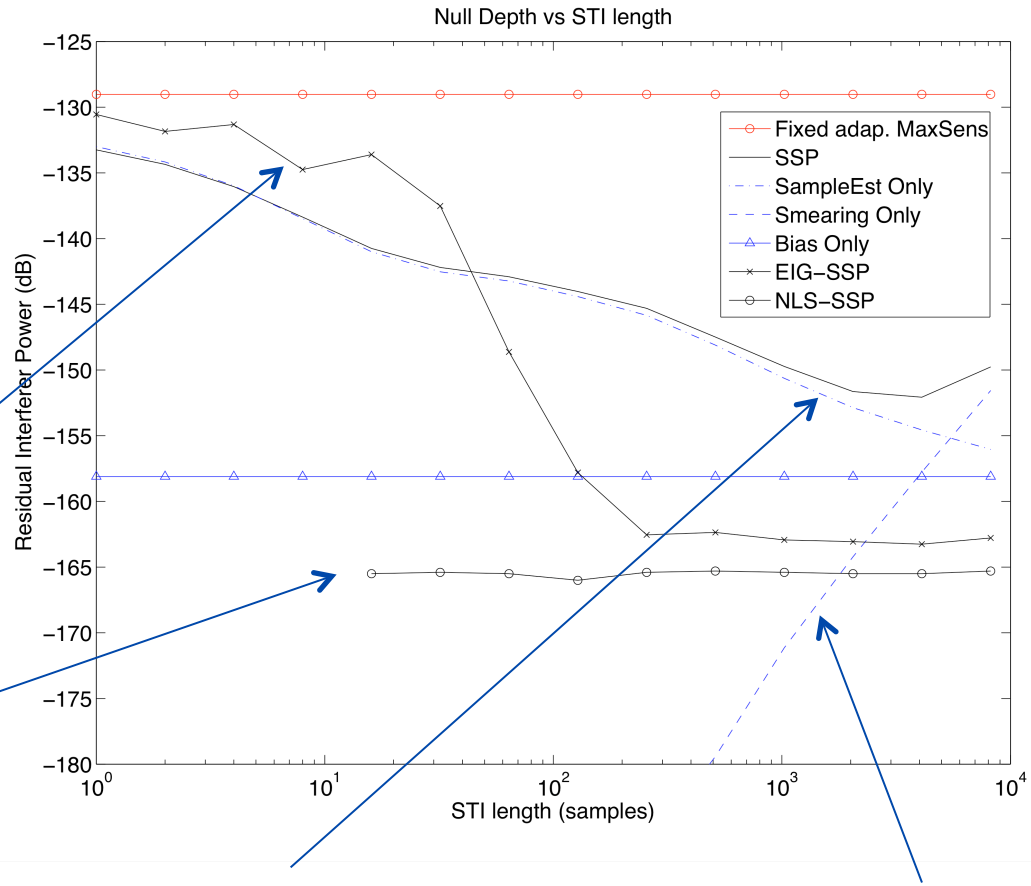

Subspace estimation error due to sample noise, i.e. null depth with no motion.

Subspace smearing error due to motion, i.e. null depth with no sample estimation error.

Conclusions and Future Work

- First demonstration of high sensitivity imaging with a PAF.
- Practical calibration and beamforming methods.
- Sensitivity, system temperature efficiency, and realized field of view match model predictions to within expected accuracy.
- Demonstration of true elevation tracking sensitivity optimization.
- Significant progress towards a truly usable adaptive PAF canceller.
- Future work:
  - Dual pol, 37 element array.
  - Real time distributed data acquisition, 5 MHz instantaneous BW.
  - Design PAF for field of view average optimal LNA noise match to reduce mutual coupling noise penalty.
  - Crycooled front ends.
  - Science-ready PAFs for Green Bank Telescope, Arecibo, SKA.
  - Apply polynomial assisted SSP to real data sets.
  - Develop polynomial smoothing for LCMV beamforming.